Journal of Non-Crystalline Solids 441 (2016) 34–41

Contents lists available at ScienceDirect

Journal of Non-Crystalline Solids

journal homepage: www.elsevier.com/locate/jnoncrysol

Glass-forming ability, sinter-crystallization behavior and microwave dielectric properties of $MgO-B_2O_3-(Al_2O_3)-SiO_2$ glass-ceramics

Sara Banijamali *, Touradj Ebadzadeh

Ceramic Department, Materials & Energy Research Center, P. O. Box: 31787-316, Alborz, Iran

ARTICLE INFO

Article history:
Received 2 January 2016
Received in revised form 13 March 2016
Accepted 17 March 2016
Available online 31 March 2016

Keywords:
Glass-ceramics
Glass-forming ability
Sinter-crystallization
Micro-structure
Dielectric properties

ABSTRACT

The present work aims to survey sinterability, crystallization behavior and microwave dielectric characteristics of $MgO-B_2O_3-SiO_2$ glass-ceramics in the presence of 1–10 weight ratios of Al_2O_3. It was shown that changing the base composition and addition of Al_2O_3 led to an increase in the glass-forming potential. Fully densified glass-ceramics were achieved by sintering below 950 °C from all selected compositions. During sintering, magnesium borate and magnesium silicate were formed in all specimens whilst cordierite was also crystallized in the specimens contained >5 weight ratios of Al_2O_3. Based on the FESEM observation, magnesium borate and magnesium silicate adopted a nanometric spherical morphology and cordierite had a platelet-like morphology. Due to the increased interface areas between crystalline phases and consequent intensified space charge polarization, addition of Al_2O_3 to the studied compositions did not affect dielectric properties, positively. However, the microwave dielectric characterization confirmed the suitability of the fabricated glass-ceramics as low-permittivity fully dense dielectric substrates.

1. Introduction

Recently, developing interest has been focused on dielectric glass-ceramics for microelectronic applications in the microwave frequency range such as LTCC (low temperature co-fired ceramics), resonators, capacitors and etc. [1–3]. This attention refers to the variety in the primary glass composition, possibility to achieve various crystalline phases with characteristic dielectric properties as well as suitable sinterability at temperatures below 950–1000 °C. In fact, concurrent formation of dielectric phases and densification through viscous flow mechanism make them appropriate candidates for the as-mentioned applications [4–8]. Among the dielectric glass-ceramic systems, $MgO-B_2O_3-SiO_2$ (MBS) ternary system presents distinguished microwave dielectric properties owing to the crystallization of magnesium borate ($Mg_2B_2O_5$) and magnesium silicate ($MgSiO_3$) crystalline phases [9–11]. Dielectric properties of the MBS glass-ceramics are comparable to those of the $CaO-B_2O_3-SiO_2$ glass-ceramics which have been commercialized as the Ferro A6 dielectric substrates for LTCC applications [12–15].

The kinetic of crystallization and phase evolution during sinter-crystallization of the MBS glass-ceramics have been explored, previously [9–10]. It was found that addition of different amounts of TiO_2 to the primary glasses of this system, promotes their crystallization and microwave dielectric properties by acting as the nucleating agent [11].

The present work aims to investigate the effects of various amounts of Al_2O_3 on sinter-crystallization and dielectric properties of the MBS glass-ceramics. To highlight the role of Al_2O_3 on crystallization tendency of the selected glass compositions, glass-forming ability of them was also examined. Al_2O_3 was chosen to enhance the crystallization of dielectric aluminosilicate phases in the glass matrix.

2. Experimental procedure

The starting glass composition (G_{base}) contained 43 wt% MgO, 35 wt% B_2O_3 and 22 wt% SiO_2 chosen from previous studies [9–11]. Al_2O_3 was then added to the base composition in amounts of 1, 3, 5, 7 and 10 weight ratios. The relevant glasses were designated as $G_{Al\text{-}1}$, $G_{Al\text{-}3}$, $G_{Al\text{-}5}$, $G_{Al\text{-}7}$ and $G_{Al\text{-}10}$, respectively.

The starting raw materials were reagent-grade chemicals of magnesium hydroxide (Merck 5870), boric acid (Merck 160), aluminum hydroxide (Merck 1093) and silica (Setabran, purity >99.8%). The homogeneous mixtures of glass batches were melted in alumina crucibles at 1350–1400 °C in an electric furnace for 3 h followed by rapid quenching in cold water to obtain frits. All frits were dry milled in an agate mortar for 45 min to reach the mean particle size of about 10 μm. Crystallization behavior of the glass frits was monitored by a differential thermal analyzer (Polymer Laboratories, STA-1640). Each DTA run was performed in air atmosphere with alumina reference sample, using a heating rate of 10 °C/min. The temperature accuracy of the DTA analysis was ±0.3 °C.

The quantitative determination of glass-forming potential of the selected compositions was carried out according to the Dietzel and

* Corresponding author.
E-mail addresses: banijamalis@yahoo.com, banijamali@merc.ac.ir (S. Banijamali).

http://dx.doi.org/10.1016/j.jnoncrysol.2016.03.014
0022-3093/

Saad-Paulin methods as Eqs. (1) and (2) [16,17]:

$$\text{Dietzel}: \quad \Delta T = (T_c - T_g) \tag{1}$$

$$\text{Saad-Paulin} \quad S = (T_c - T_x)(T_x - T_g)/T_g. \tag{2}$$

In these equations, T_c, T_x and T_g are respectively referred to the crystallization peak, onset of the crystallization peak and glass transition temperatures which are extracted from the relevant DTA thermograph for each glass composition. Enhancement of the factors ΔT and S means the increase of glass-forming ability or resistance against crystallization.

Glass frits were mixed by 0.1 wt% CMC (carboxymethyl cellulose) and uniaxially pressed under initial pressure of 30 MPa and final pressure of 70 MPa to obtain compacted glass pellets with 1 cm in diameter. Glass pellets were subjected to the one-step simultaneous sinter-crystallization heat treatment at the temperature interval of 700–1000 °C to obtain glass-ceramic specimens. Crystalline phases precipitated during heat treatment were identified by X-ray diffractometer (Siemens D500) with Cu-K_α radiation. Prior to diffractometry, glass-ceramic specimens were pulverized to reach the particle size of <75 μm.

Sinterability of the glass-ceramic specimens was evaluated by measuring water absorption and bulk density. The glass-ceramic samples after polishing and etching (in a 5 vol% HF solution for a few seconds) were coated by a thin layer of gold and subjected to the FESEM analysis (field emission scanning electron microscope, Zeiss). The FESEM instrument was equipped with an energy dispersive analysis of X-ray (EDAX) capability. The EDAX detector was not capable to detect boron in the examined specimens.

Dielectric features of the optimized sintered glass-ceramics including permittivity (ε_r), resonance frequency (f_r) and dielectric loss tangent (tanδ) were evaluated by a network analyzer (HP 8510-C) in the frequency range of 8–12 GHz.

3. Results and discussion

3.1. Glass-forming ability measurement

Fig. 1 represents the DTA thermographs of the studied glass frits. Based on Fig. 1, only one crystallization peak temperature is detectable for each fabricated glass. By addition of Al_2O_3 to the base glass (G_{base}) and increasing its content, the crystallization peak shifts to higher temperatures, considerably. However, the glass transition (T_g) and dilatometric softening point temperatures (T_d) are slightly increased (as shown in Table 1). Since all glasses possess the same viscosity at the glass transition temperature ($10^{12.5}$ Poise), it seems that Al_2O_3 has not affected the glass viscosity, noticeably.

To explore the effect of Al_2O_3 on glass-forming potential and structure of the studied glasses, the glass-forming ability was measured according to the Dietzel and Saad-Paulin methods and collected in Table 1. It was found that by addition and increase of Al_2O_3, the glass-forming ability is obviously increased. According to the obtained results, it can be suggested that Al_2O_3 has acted as a network former oxide by contributing as the [AlO_4] tetrahedron into the glass structure. In fact, when Al^{3+} cations occupy the tetrahedral positions decrease the glass dissociation and increase its resistance against crystallization by introducing only 1.5 oxygens per network-forming cation and converting non-bridging oxygens to bridging ones. Therefore, the glass $G_{Al\text{-}10}$ has the best glass-forming behavior among the studied glasses.

To identify the crystalline phases precipitated at the crystallization peak temperature, each glass (powder sample) was heat treated at its crystallization temperature extracted from the DTA thermograph for 15 min, separately. Fig. 2 depicts the XRD patterns of the specimens heat treated at their crystallization peak temperature. As it can be observed, magnesium borate ($Mg_2B_2O_5$) is crystallized in all heat

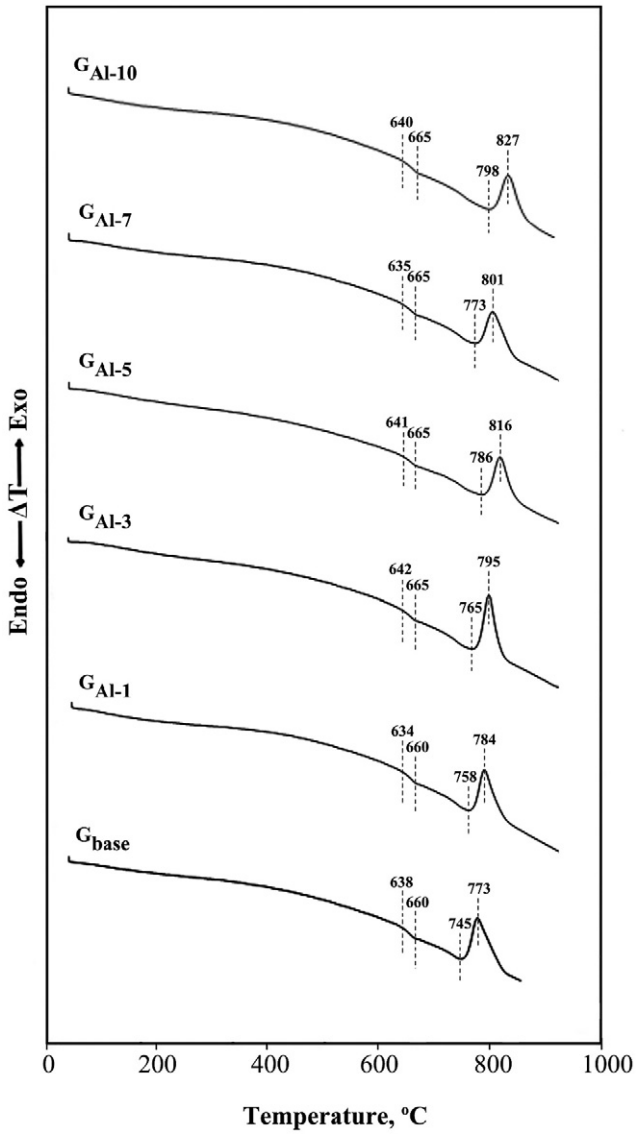

Fig. 1. DTA thermographs of the studied glasses at the heating rate of 10 °C/min.

treated glasses and no evidence of Al_2O_3 bearing crystalline phases is detectable. Apparently, Al_2O_3 has been remained in the residual glass matrix of the crystallized specimens.

To have a better quantitative understanding of crystallinity, the variation of magnesium borate intensity versus glass composition was plotted as Fig. 3 (in this measurement, the strongest peak line of magnesium borate was considered at the two theta position of 34.6). According to this figure, magnesium borate crystallinity is continuously declined by increasing of the Al_2O_3 content. This result is in agreement with the glass-forming potential measurement. Therefore, it can be concluded

Table 1
Characteristic temperatures of the DTA thermographs and glass-forming ability measurements.

Glass	T_g (±0.3 °C)	T_d (±0.3 °C)	T_x (±0.3 °C)	T_c (±0.3 °C)	S (±0.3 °C)	ΔT ($T_c - T_g$) (±0.3 °C)
G_{base}	638	660	745	773	4.69	135
$G_{A1\text{-}1}$	634	660	758	784	5.09	150
$G_{A1\text{-}3}$	642	665	765	795	5.75	153
$G_{A1\text{-}5}$	641	665	786	816	6.79	175
$G_{Al\text{-}7}$	635	665	773	801	6.09	166
$G_{A1\text{-}10}$	640	665	798	827	7.16	187